

A novel silent mutation E83E of α A-crystallin in age-related cataract with impaired chaperone function

Fanqian Song

Eye Hospital, First Affiliated Hospital, Harbin Medical University <https://orcid.org/0000-0002-3509-2529>

Dongrui Liu

Eye Hospital, First Affiliated Hospital, Harbin Medical University

Liyao Sun

Eye Hospital, First Affiliated Hospital, Harbin Medical University

Chao Wang

Eye Hospital, First Affiliated Hospital, Harbin medical university

Xi Wei

Eye Hospital, First Affiliated Hospital, Harbin Medical University

Hanruo Liu

Beijing Institute of Ophthalmology, Beijing Tongren Hospital, Capital Medical University, Beijing Ophthalmology&Visual Science Key Lab Affiliated Anzhen Hospital

Xianling Tang

Eye Hospital, First Affiliated Hospital, Harbin Medical University

Hongyan Ge (✉ gehongyan@hrbmu.edu.cn)

Eye Hospital, First Affiliated Hospital, Harbin Medical University

Ping Liu (✉ ping_liu53@hotmail.com)

First Affiliated Hospital, Harbin Medical University

Research article

Keywords: age-related cataract, CRYAA, mutation, chaperone function

Posted Date: June 5th, 2020

DOI: <https://doi.org/10.21203/rs.3.rs-29161/v1>

License:   This work is licensed under a Creative Commons Attribution 4.0 International License.

[Read Full License](#)

Abstract

Background

Age-related cataract (ARC) is the leading cause of blindness of the aged, influenced by environmental factors and genetic factors. However, it is scanty in gene mutation studies. The study aims to expand knowledge of etiology of ARC.

Methods

Peripheral blood samples of ARC patients were collected to screen α A-crystallin (CRYAA) gene mutations by single strand conformation polymorphism assay. Cell morphology, protein expression level and chaperone function of CRYAA in HLE B-3 cell line influenced by mutant CRYAA were next analyzed. Chaperone function of mutant CRYAA was measured by aggregation assay in physiological status, heat treatment (42°C) and ultraviolet (UV) treatment. Cell morphology and protein expression level effected by UV in human lens epithelial B3 (HLE B-3) cells and human anterior lens capsules (ALCs) were further analyzed.

Results

We identified a novel silent mutation in CRYAA (c.249G > A, p.E83E) among 300 ARC patients. CRYAA-E83E may up-regulate the CRYAA expression levels of both mRNA and protein, and change the distribution of CRYAA in HLE B-3 cells. Compared to wild type CRYAA (CRYAA-WT), CRYAA-E83E showed lower chaperone function after 42°C heat treatment and UV treatment. Meanwhile, after UV treatment, HLE B-3 cells and lens epithelial cells in human ALCs showed irregular and flatten morphology; decreased CRYAA expression levels; increased laminin γ 2 expression levels, and changed epithelial-mesenchymal transition (EMT) related protein expression levels.

Conclusions

The E83E mutation of CRYAA is a potential pathogenic mutation, considering its influence on the expression level, intracellular distribution and chaperone function of CRYAA.

Background

Cataract is a leading cause of blindness worldwide. It is an irreversible eye disease results from loss of transparency of crystalline. About 80% cataracts are age-related, defined as age-related cataract (ARC). The formation of ARC is multi-factorial, and epidemiology research showed both environmental factors (such as oxidative stress, thermal injury, and UV irradiation) and genetic factors playing an important role [1,2].

The α -Crystallin is a major structural and refractive protein in the vertebrate lens [3, 4] and belongs to the small heat shock protein family [5]. The two subunits, α A and α B have 57% sequence homology [6]. α A-crystallin (CRYAA) comprises of 173 amino acid residues, has a molecular mass of 20 kDa, is encoded by CRYAA gene and is found almost exclusively in the lens tissues [7]. CRYAA gene is located in chromosome 21 comprised of 3 exons. CRYAA has the chaperone function like other heat shock proteins and plays an important role in prevention of various substrate protein aggregation induced by UV and maintaining transparency of lens [8,9]. CRYAA is divided into 3 functional domains artificially: N-terminal domain (residues 1-143), α -crystallin domain (residues 64-144) and C-terminal domain (residues 145-173) [10]. It has been reported that residues 70-88 in CRYAA acted as a primary substrate binding site and account for the bulk of the total chaperone activity [11].

Several mutations of CRYAA gene have been reported to be related with ARC such as D2D, R54K, R65Q and F71L [12-15]. Up to now, D2D mutation is known to be the only silent mutation in the coding region of CRYAA associated with congenital and age-related cataract. The silent mutation of D2D results in a compact CRYAA mRNA secondary structure compared to wild type CRYAA mRNA [12]. Meanwhile, more research proves silent mutations might influence the process of transcription, protein structure or protein function [16,17].

It has been known for a long time that heat treatment affected the expression, structure and function of heat shock proteins including CRYAA [18-20]. CRYAA had increased membrane-bound fractions when cells were treated with heat shock at 42°C detected by immunoblotting (IB) [21]. The results suggested that the altered distributions in cellular of CRYAA might contribute to the onset of ARC. In the process of ARC, the accumulated various stresses and some mutations might affect the cellular distributions and cellular functions of CRYAA [21].

Lens tissues are formed by the proliferation and differentiation of the lens epithelial cells. Recently, human anterior lens capsules (ALCs) models in vitro was constructed successfully using the human lens epithelial B3 (HLE B-3) cell line basement membrane (BM) [22]. Cells transfected with CRYAA indicated its ability to prevent UVA induced apoptosis in human lens epithelial cells [23-25].

Epithelial-mesenchymal transition (EMT) has been widely studied in the posterior cataract, but there's no report showed the relationship between EMT and ARC. In vitro experiments showed that UVB could up-regulate expression levels of Orthodenticle Homeobox 2 (Otx2) in SRA cell lines, and the increased Otx2 induced EMT and up-regulated Smooth muscle actin (SMA) [26]. Laminin γ 2 is an important structural component of the epithelial BM in various normal tissues [27].

In the present study, we identified a novel silent mutation E83E of CRYAA among 300 ARC patients. And further investigation was performed to study their potential contribution to the pathogenesis of ARC.

Methods

Peripheral blood samples collection and DNA extraction

A total of 300 nuclear ARC patients (aged 21–92 years old) and 100 unrelated normal subjects (aged 0–39 year old) were recruited from the First Affiliated Hospital of Harbin Medical University (Harbin, China). Peripheral blood samples were collected using EDTA tubes and stored at -20°C. The genomic DNA was extracted by TIANGEN Genomic DNA Kit (TIANGEN, Beijing, China). This study was approved by the Internal Review Board of Harbin Medical University. All the experiments were conducted in accordance with Declaration of Helsinki Principles. Informed consents were obtained from all individuals involved.

Polymerase chain reaction (PCR)

PCR amplification was performed with 50 ng of genomic DNA in a 25 µl reaction mixture containing 12.5 µl of 2 × PrimeSTAR Max Premix (Takara Bio Inc., Dalian, China), 0.2 µM of each primer. The PCR products were run on 1.5% agarose gel. The primers used were listed in Table 1.

Single strand conformation polymorphism (SSCP) and sequencing

Double-stranded DNA is denatured to single-stranded DNA in the technology of SSCP. Mutation screening was carried out by SSCP analysis as described previously [9]. PCR products of affected individuals were purified and sequenced by HaiGene (Harbin, China).

Cell culture

HLE B-3 stable cell line was obtained from the American Type Culture Collection (Manassas, VA, USA) and cultured as previously described [28,29].

Plasmid transfection

The plasmids of blank vector [pcDNA3.1(+)], wildtype CRYAA (CRYAA-WT) and CRYAA-E83E were obtained from BSGens Company (Harbin, China). HLE B-3 cells were seeded in 6-well plates and were transfected with 2 µg/well pcDNA3.1(+), CRYAA-WT and CRYAA-E83E plasmids using Invitrogen Lipofectamine® 2000 Reagent (Thermo Fisher Scientific Inc., Shanghai, China) as described previously [28,29].

Reverse transcription-PCR (RT-PCR)

CRYAA (NM_001363766.1) mRNA levels were analyzed by RT-PCR. Total RNA was isolated from HLE B-3 cells transfected with CRYAA-WT and CRYAA-E83E plasmid using TRIZOL reagent (HaiGene) according to the manufacturer's protocol. RNA (1 µg) was reverse transcribed using PrimeScript™ II Reverse Transcriptase (Takara Bio Inc.) according to the manufacturer's protocol. PCR was performed with 5 µl of RT product, in a 25 µl reaction mixture containing 0.625 U of TaKaRa Ex Taq (Takara Bio Inc.) and 0.2 µM of each primer. The PCR products were run on 1.5% agarose gel and visualized by staining with Ethidium Bromide (Sigma Aldrich; Merck KGaA). GAPDH (NM_001256799.3) was used as an internal control. The primers used were listed in Table 1.

Antibodies

Rabbit polyclonal antibody (pAb) against CRYAA(catnos.abs116815, Absin), rabbit pAb against laminin γ 2 (catnos.C30224, Assay Biotechnology Company), rabbit pAb against fibronectin(catnos. 15613-1-AP, proteintech), rabbit pAb against α -SMA (catnos.Ab5694, Abcam), mouse monoclonal antibody (mAb) against β -actin(cat nos. AF0003, Beyotime Institute of Biotechnology), mouse mAb against GAPDH (cat nos. AF0006, Beyotime Institute of Biotechnology), mouse mAb against histone H3 (catnos.AF0009, Beyotime Institute of Biotechnology), mouse mAb against bcl-2 (catnos. sc-7382, Santa Cruz Biotechnology) and rabbit pAb against bax(cat nos. 50599-2-Ig, proteintech) were used in the present study.

IB

Protein levels of CRYAA, histone H3, GAPDH, α -SMA, laminin γ 2, fibronectin (FN), bax, bcl-2 in HLE B-3 cell lysates, supernatants, BMs and human ALCs were analyzed by IB. After plasmid transfection for 48 h, HLE B-3 cell lysates, supernatants and BMs were harvested as described previously [25]. Human ALCs lysates were collected as described below.

Chaperone function assay

Aggregation assay was chosen as the method to evaluate the chaperone function of CRYAA as described previously [19]. HLE B-3 cells transfected with CRYAA-WT and CRYAA-E83E plasmids were grown to 100% confluency in a 6-well plate. Cell lysates were collected, 100 μ l lysates containing equal amounts of proteins were incubated at 55°C in water bath for 3 h for protein aggregation. Soluble and insoluble fractions were separated by centrifuge with 18,000 \times g/ 10 min at 4°C. The supernatant was as the soluble section. Sediment was dissolved by 25 μ l 2 \times sample buffer as the insoluble section. The expression level of client proteins was detected by IB as described above.

Preparation of nuclear and cytoplasmic protein

HLE B-3 cells were seeded in 6-well plates and were transfected with 2 μ g/well CRYAA-WT and CRYAA-E83E plasmids. The nuclear and cytoplasmic proteins were extracted by Nuclear and Cytoplasmic Protein Extraction Kit (Beyotime Institute of Biotechnology, Shanghai, China) according to the manufacturer's protocols.

HLE B-3 cells treated with 42 °C

The 42°C treatment assay was performed as described previously [25]. Briefly, HLE B-3 cells transfected with plasmids were cultured in 6-well plates and put into humidified atmosphere with 5% CO₂ for 24 h. Cells were cultured at 42°C in humidified atmosphere without CO₂ for 4 h. With those cultured at 37°C in humidified atmosphere without CO₂ for 4 h as negative control. Cells lysates were collected as described above.

HLE B-3 cells treated with UV

HLE B-3 was cultured in 6-well plate grown to 95% confluency. Cell supernatant was discarded and washed with PBS twice, 500 μ l PBS was kept in each well. Cells were exposed to UV (253.7 nm, 100 μ W/cm²) for 1 h.

For negative control, cells were kept at room temperature in PBS without UV irradiation for 1 h. HLE B-3 cells transfected with plasmids were cultured in low-glucose DMEM containing 10% FBS at 37°C in humidified atmosphere with 5% CO₂ for 24 h. Cells were then treated with UV for 1 h as described above. HLE B-3 cell lysates, supernatants and basement membranes were harvested as described previously [25].

Human ALCs collection and treated with UV

Cataract severity of nuclear ARC were graded by the Emery-Little Classification System of nuclear opacity grade before surgery. Human ALCs of nuclear grade Ⅲ were collected from 20 individuals with ARC at the First Affiliated Hospital of Harbin Medical University (Harbin, China). Human ALCs were obtained using the central circular capsulorhexis method by a single ophthalmologist during surgery. Human ALCs were stored in low-glucose DMEM at 4°C and immediately transferred to laboratory. Human ALCs were cut into 2 pieces at the same size and tiled in two 35-mm dish containing 750 μl PBS respectively. One dish was treated by UV (253.7 nm, 100 μW/cm²) for 30 min. After treated, changed PBS with 1.5 ml low-glucose DMEM containing 10% FBS, 100 units/ml penicillin and 100 μg/ml streptomycin. Human ALCs were cultured at 37°C with 5% CO₂ for 24 h. The UV group was again treated with UV for 30 min, turned-over each pieces of ALCs and treated another 30 min with UV. Another one dish without treated as the negative control. Lysates of human ALCs was prepared as described previously [22].

Coomassie brilliant blue (CBB) staining

HLE B-3 basement membranes were separated by 10% SDS-PAGE, then stained by CBB staining R250 as described previously [25].

Statistical analysis

Statistical analysis was performed using SPSS 18.0 (SPSS, Inc., Chicago, IL, USA). The quantitative data are shown as mean ± standard deviation. *P* values less than 0.05 were considered as statistically significant.

Results

Screening and identification of CRYAA mutations in ARC patients

Genomic DNA samples were isolated from peripheral blood samples of 300 ARC patients and 100 normal subjects. The SSC Passay showed mobility shift pattern in a 63-year-old male ARC patient (S220) in exon 2 of CRYAA gene (Fig. 1A). Such changes were not observed among 100 normal controls. Sequencing of amplified products revealed a novel heterozygous G > A nucleotide substitution in exon 2 of CRYAA (c.249G > A, NG_009823.1), which did not change the amino acid sequence (Glutamic acid, Glu) at codon 83 (p.E83E) (Fig. 1B). The Glu83 of CRYAA gene are highly conserved among 8 species (Fig. 1C).

Protein expressions, distribution and chaperone function influenced by CRYAA-E83E

We construct CRYAA-WT and CRYAA-E83E plasmids to investigate the function of the novel silent mutation of CRYAA-E83E. In HLE B-3 cells, compared to blank vector, transfection of CRYAA-WT and CRYAA-E83E

showed significant increased CRYAA gene (Fig. 2A) and protein (Fig. 2B) expression levels by RT-PCR and IB, respectively; compared to CRYAA-WT, CRYAA-E83E showed higher expression levels of CRYAA gene and protein levels detected by RT-PCR (Fig. 2A) and IB (Fig. 2B), respectively. To investigate the protein distribution of CRYAA, protein expression levels influenced by CRYAA-E83E in nuclear and cytoplasmic proteins of HLEB-3 cells were analyzed. Histone H3 was used as internal reference of nuclear proteins. β -actin was used as internal reference of cytoplasmic proteins. Compared to blank vector, the expression levels of CRYAA contributed by CRYAA-WT and CRYAA-E83E were significantly higher in nucleus and cytoplasm. Compared to CRYAA-WT, the protein expression levels of CRYAA by CRYAA-E83E was lower in both nuclear and cytoplasmic lysates (Fig. 2C).

CRYAA is widely regarded as the small heat shock protein which mainly suppress the aggregation of different client proteins. CRYAA-WT and CRYAA-E83E plasmids were transfected into HLEB-3 cells. Cell lysates were centrifuged into soluble and insoluble fractions, the insoluble fraction indicates the expression level of aggregated client proteins. Aggregation of GAPDH, α -SMA, FN, laminin γ 2 proteins in HLE B-3 cell lysates were detected by IB. Compared to blank vector, HLE B-3 cells transfected with CRYAA-WT showed higher expression levels of total, soluble and insoluble CRYAA detected by IB; compared to CRYAA-WT, HLEB-3 cells transfected with CRYAA-E83E showed higher soluble CRYAA expression levels and similar insoluble CRYAA expression levels (Fig. 2D). Compared to blank vector, HLEB-3 cells transfected with CRYAA-WT showed similar total, soluble and insoluble GAPDH expression levels; compared to CRYAA-WT, HLEB-3 cells transfected with CRYAA-E83E showed similar total GAPDH expression levels, lower soluble GAPDH expression levels and similar insoluble GAPDH expression levels (Fig. 2D). Compared to blank vector, HLEB-3 cells transfected with CRYAA-WT showed similar total, soluble and insoluble α -SMA expression levels; compared to CRYAA-WT, HLEB-3 cells transfected with CRYAA-E83E showed similar total α -SMA expression levels, lower soluble and insoluble α -SMA expression levels (Fig. 2D). Compared to blank vector, HLEB-3 cells transfected with CRYAA-WT showed higher total FN expression levels, lower soluble FN expression levels and higher insoluble FN expression levels; compared to CRYAA-WT, HLE B-3 cells transfected with CRYAA-E83E showed lower total FN expression levels, higher soluble FN expression levels and lower insoluble FN expression levels (Fig. 2D). Compared to blank vector, HLEB-3 cells transfected with CRYAA-WT showed similar total, soluble and insoluble laminin γ 2 expression levels; compared to CRYAA-WT, CRYAA-E83E had similar total, soluble and insoluble laminin γ 2 expression levels (Fig. 2D).

Morphology and chaperone function influenced by CRYAA-E83E treated with 42°C

To further investigate the chaperone function influenced by CRYAA-E83E, HLE B-3 cells transfected with CRYAA-WT and CRYAA-E83E plasmid were cultured in medium at 37°C for 24 h, then changed into 42°C for 4 h, with those cultured at 37°C for 4 h as negative control. After treated, cells shranked, became small and turned round, and vacuoles were located around the cells (Fig. 3A). Aggregation of CRYAA and GAPDH were detected by IB through chaperone function. Compared to blank vector, the expression levels of total, soluble and insoluble CRYAA were higher in HLE B-3 cells transfected with CRYAA-WT and CRYAA-E83E; compared to CRYAA-WT, HLE B-3 cells transfected with CRYAA-E83E showed lower

soluble CRYAA expression levels and higher insoluble CRYAA expression levels (Fig. 3B). Compared to blank vector, HLEB-3 cells transfected with CRYAA-WT showed similar total and soluble GAPDH expression levels, slightly lower insoluble GAPDH expression levels; compared to CRYAA-WT, HLE B-3 cells transfected with CRYAA-E83E showed similar total GAPDH expression levels, lower soluble GAPDH expression levels and higher insoluble GAPDH expression levels (Fig. 3B).

Morphology and protein expression in HLE B-3 cells and human anterior lens capsules treated by UV

To investigate the influence of UV treatment on morphology and protein expressions of HLE B-3 cells, cells were treated with UV for 30 min or 1 h, with cells without treatment as negative control. After UV treatment, HLE B-3 cells became irregular in shape and flatten, particularly those treated with UV for 1 h (Fig. 4A). In the early stage (UV 30 min), apoptosis with nuclear chromatin condensation and fragmentation as well as apoptotic bodies were observed (Fig. 4A). In the late stage (UV 1 h), cells became more flatten, and the apoptotic cells might be phagocytized by adjacent cells (Fig. 4A). Compared to cells without UV treatment, HLE B-3 cells treated with UV showed lower expression levels of CRYAA, FN and α -SMA, and higher expression levels of laminin γ 2 and N-cadherin by IB (Fig. 4B).

We further collected human ALCs of nuclear grade \leq from 20 ARC patients. Human ALCs were treated with UV for 1 h and cultured in medium at 37°C for another 24 h, and then treated with UV again for 30 min. Human ALCs without treatment were as negative control (without). A large number of lens epithelial cells under anterior capsules were observed. Cells became irregular, flatten and vacuolization, the nucleus boundaries were unclear, which is similar to the changes of HLE B-3 cells treated with UV. Cell apoptosis was induced (Fig. 4C). IB of human ALCs showed lower expression levels of CRYAA and N-cadherin, and higher expression levels of laminin γ 2 after treated with UV (Fig. 4D).

Morphology and chaperone function influenced by CRYAA-E83E treated with UV

To further investigate the chaperone function influenced by CRYAA-E83E at different conditions, CRYAA-WT and CRYAA-E83E plasmids were transfected into HLE B-3 cells. Then treated HLE B-3 cells with UV for 30 min, cells without treatment as negative control. HLE B-3 cells without any treatment and cells transfected with blank vector became irregular and flatten after treated with UV. A large number of apoptotic bodies were observed in HLE B-3 cells transfected with CRYAA-WT and CRYAA-E83E after UV treatment (Fig. 5A). In HLE B-3 cells treated with UV for 30 min, compared to blank vector, cells transfected with CRYAA-WT and CRYAA-E83E showed significantly higher CRYAA expression levels; compared to CRYAA-WT, the expression levels of CRYAA contributed by CRYAA-E83E were higher (Fig. 5B). Compared to blank vector, Bcl-2/Bax ratio by CRYAA-WT was higher, suggesting CRYAA-WT might have function of anti-apoptosis; compared to CRYAA-WT, HLE B-3 cells transfected with CRYAA-E83E showed higher Bcl-2/Bax ratio (Fig. 5B), suggesting CRYAA-E83E mutation might increase the ability of anti-apoptosis. Aggregation of CRYAA and GAPDH protein in HLE B-3 cell lysates were detected by IB through chaperone function assay. Results showed that, compared to blank vector, the expression levels of total CRYAA were higher contributed by CRYAA-WT and CRYAA-E83E; compared to CRYAA-WT, the expression levels of total, soluble and insoluble CRYAA were higher by CRYAA-E83E (Fig. 5C). Compared to blank vector, HLE B-

3 cells transfected with CRYAA-WT showed similar total, soluble and insoluble GAPDH expression levels; compared to CRYAA-WT, HLE B-3 cells transfected with CRYAA-E83E showed lower soluble GAPDH expression levels and higher insoluble GAPDH expression levels (Fig. 5C). Suggesting the impaired chaperone function of CRYAA-E83E. To investigate the expression levels of histone H3, we collected BM of HLE B-3 cells treated with UV for 30 min, with BM without treated as negative control. In the BM of untreated HLE B-3 cells, compared to blank vector, the expression levels of histone H3 contributed by CRYAA-WT were lower; compared to CRYAA-WT, the expression levels of histone H3 by CRYAA-E83E were similar (Fig. 5D). CBB staining (bottom) of BM proteins was used to be internal reference (Fig. 5D). In the HLE B-3 cell BM treated with UV, the expression levels of histone H3 level by CRYAA-E83E were significantly up-regulated (Fig. 5D). To investigate the expression levels of secretory CRYAA, CRYAA-WT and CRYAA-E83E plasmids were transfected into HLE B-3 cells. After treated with UV for 30 min, the supernatant of HLE B-3 cells was collected, with supernatant without treated as negative control. In the supernatant of HLE B-3 cells, compared to blank vector, the expression levels of CRYAA were higher contributed by CRYAA-WT and CRYAA-E83E; compared to CRYAA-WT, the expression levels of CRYAA by CRYAA-E83E were lower before treated, but higher after treated with UV for 30 min (Fig. 5E).

Discussion

In the present study, we found a novel silent heterozygous G > A nucleotide mutation in exon 2 of CRYAA (c.249G > A, p.E83E) in an old male (S220) case among 300 ARC patients. The age-at-onset of cataract was 63 in S220 considered as early onset of ARC in view of the mean age of ARC cases (64.3 ± 12.9). To the best of our knowledge, CRYAA-E83E and CRYAA-D2D were the only two silent mutations in the coding region of CRYAA related to ARC. The expression levels, distributions and chaperone functions of CRYAA influenced by CRYAA-E83E were investigated in the present study.

The expression levels of CRYAA gene and protein were up-regulated in HLE B-3 cell lysates contributed by CRYAA-E83E, prompting that silent mutation did not change the amino acid sequence, but, influence processes of transcription and translation.

Karen L found the recombinant exogenous proteins were co-localized with the native CRYAA in perinuclear regions detected by immunohistochemistry [30]. The altered distributions in cellular of CRYAA might contribute to the onset of ARC [21]. In the present study, the distribution of CRYAA were more in cytoplasm than nucleus in HLE B-3 cell lysates transfected with CRYAA-WT. The increased CRYAA located in cytoplasm may act as a functional protein. Compared to CRYAA-WT, the expression level of CRYAA was less both in HLE B-3 cell nucleus and cytoplasm transfected with CRYAA-E83E, we proposed it may mainly distribute on the cytomembrane, but more experiments need to be done. Histone H3 was widely used as internal control in nuclear protein. Results showed histone H3 also expressed in the cytoplasm of HLE B-3 cells in the present study.

It has been reported that the lens fiber cell marker gene CRYAA was decreased in process of EMT [31]. However, whether CRYAA influenced the expression of EMT marker genes has never been reported.

In the present study, CRYAA-WT promoted the expression of FN, while mutant CRYAA had part of these functions. We proposed that reduced FN induced by UV may be regulated by CRYAA, but more experiments still need to be done. Over-expression of CRYAA-WT did not influence the expression of α -SMA and laminin γ 2 in the present study.

It has been reported that the chaperone activity decreased 50% with deletion of residues 70–76, whereas loss of 100% chaperone-like activity with deletion of residues 70–88 when Adipic acid dihydrazide was used as the substrate protein [17]. The mutation at codon 83 (E83E) was included in the residues 70–88, which were reported as the main chaperone-like activity area in CRYAA [17]. Chaperone function measured at the temperature of physiological showed CRYAA were more insoluble fraction of HLE B-3 cell lysate contributed by CRYAA-E83E. It did not show better chaperone function against aggregation of GAPDH, α -SMA and laminin γ 2 by CRYAA-WT at the physiological temperature as described previously [32]. Compared to CRYAA-WT, chaperone function influenced by CRYAA-E83E showed the ability to promote GAPDH aggregation; suppress α -SMA and FN aggregation; no influence against laminin γ 2 aggregation. Chaperone function measured by aggregation assay influenced by 42°C treatment and UV irradiation were first constructed in this study. The heat treatment response occurred in HLE B-3 cells after treated with 42°C for 4 h. HLE B-3 cell lysates transfected with CRYAA-WT treated with 42°C showed little impact on chaperone function; HLE B-3 cell lysates transfected with CRYAA-E83E treated with 42°C showed decreased chaperone function against GAPDH aggregation,

UV has been proved to up-regulate the expression level of EMT-related molecules, such as FN, α -SMA and N-cadherin [26,33,34]. UV could also down-regulate the expression level of lens fiber cell marker gene CRYAA in lens epithelial cells of mouse [26]. Laminin γ 2 promoted metastasis in lung adenocarcinoma via EMT [31]. We identified UV could induce apoptosis of HLE B-3 cells. In the present study, the expression levels of laminin γ 2 and N-cadherin were higher and the expression levels of FN, α -SMA and CRYAA were lower after treated with UV in HLE B-3 cell lysates. The reason of down-regulation of FN and α -SMA needs to be further explored. The expression levels of laminin γ 2 and N-cadherin in UV treated human ALCs have never been reported. After treated with UV, human lens epithelial cells showed similar changes in morphology (became irregular and flatten) with HLE B-3 cell line. The present study showed decreased CRYAA expression level and increased laminin γ 2 expression level in human ALCs, which were similar with HLE B-3 cells treated with UV. But the increased N-cadherin expression level was opposite to HLE B-3 cells treated with UV.

HLE B-3 cells transfected with CRYAA-WT and CRYAA-E83E plasmids were treated with UV for 30 min. The Bcl-2/Bax ratio from high to low was CRYAA-E83E, CRYAA-WT, normal and blank vector, proved the stronger anti-apoptosis function influenced by CRYAA-WT and CRYAA-E83E. HLE B-3 cell lysates transfected with CRYAA-WT treated with UV showed little impact on chaperone function; HLE B-3 cell lysates transfected with CRYAA-E83E treated with UV showed decreased chaperone function against GAPDH aggregation, which were similar to results treated with 42°C. It has been reported the HLE B-3 cell line BM constructed as human ALCs models in vitro [22]. In BM of HLE B-3 cells transfected with CRYAA-WT and CRYAA-E83E plasmids, the expression levels of histone H3 were similar before UV treated in the present

study. The expression levels of histone H3 were upregulated by CRYAA-E83E after treated with UV, suggesting increased expression levels of histone H3 in ARC patients' ALCs. Compared to CRYAA-WT, the expression level of secretory CRYAA by CRYAA-E83E were lower before UV treatment and upregulated after UV treatment.

In summary, HLE B-3 cells transfected with CRYAA-E83E showed up-regulated expression levels of CRYAA; changed distributions of CRYAA in cells; impaired chaperone function after 42°C heat treatment and UV irradiation. Genetic factors of CRYAA-E83E mutation and environmental factors of heat treatment and UV irradiation were possible underlying mechanisms in ARC.

Conclusions

CRYAA-E83E silent mutation up-regulated the expression level of CRYAA; changed distributions of CRYAA and histone H3 in cells; impaired the chaperone function of CRYAA after 42°C heat treatment and UV irradiation. Meanwhile, UV induced cell apoptosis and decreased the expression level of CRYAA in HLE B-3 cells and human lens anterior capsules, might be an important aspect in the pathogenesis of ARC.

Abbreviations

ARC: age-related cataract; CRYAA: α A-crystallin; UV: ultraviolet; HLE B-3 cells: human lens epithelial B3 cells; CRYAA-WT: wild type CRYAA; EMT: epithelial-mesenchymal transition; IB: immunoblotting; BM: basement membrane; Otx2: Orthodenticle Homeobox 2; SMA: Smooth muscle actin; PCR: polymerase chain reaction; SSCP: single strand conformation polymorphism; RT-PCR: reverse transcription-PCR; pAb: polyclonal antibody; mAb: monoclonal antibody

Declarations

Acknowledgements

Not applicable.

Author Contributions

P.L., X.L.T., H.Y.G. designed this study. F.Q.S., D.R.L., L.Y.S., C.W., X.W., H.R.L., X.L.T. and H.Y.G. harvest samples and performed the experiments. F.Q.S. wrote the manuscript. P.L., H.Y.G. and X.L.T. revised the manuscript. All authors have read and approved of the final version.

Funding

This study was supported by the Heilongjiang Provincial Natural Science Foundation of China (H2017028); the Nature Science Foundation of China (81470618), and the National Natural Science Fund Projects of China (81271005). The funding organizations had no role in designing or conducting of this research.

Availability of data and materials

The datasets used and/or analyzed during the current study are available from the corresponding author on reasonable request.

Ethics approval and consent to participate

This study was approved from the Internal Review Board of Harbin Medical University and followed the tenets of Declaration of Helsinki. Written informed consent was obtained from all the participants and from a parent or guardian for participants under 18 years old after complete explanation.

Consent for publication

The potentially identifiable data was consented to publish by all the participants and the parent or guardian for participants under 18 years old.

Competing interests

The authors have declared that no competing interests exist.

References

1. Congdon NG, Friedman DS, Lietman T. Important causes of visual impairment in the world today. *JAMA*. 2003;290:2057–60.
2. Brian G, Taylor H. Cataract blindness—challenges for the 21st century. *Bull World Health Organ*. 2001;79(3):249–56.
3. Bloemendal H. The vertebrate eye lens. *Science*. 1977;197:127–38.
4. Delaye M, Tardieu A. Short-range order of crystallin proteins accounts for eye lens *Transparency*. *Nature*. 1983;302:415–7.
5. Ingolia TD, Craig EA. Four small Drosophila heat shock proteins are related to each other and to mammalian alpha-crystallin. *Proc Natl Acad Sci USA*. 1982;79:2360–4.
6. Van Der Ouderaa FJ, De Jong WW, Hilderink A, Bloemendal H. The amino-acids sequence of the alphaB2 chain of bovine alpha-crystallin. *Eur J Biochem*. 1974;49(1974):157–68.
7. Deretic D, Aebersold RH, Morrison HD, Papermaster DS. AlphaA- and alpha B-crystallin in the retina. Association with the post-Golgi compartment of frog retinal photoreceptors. *J Biol Chem*. 1994;269(24):16853–61.
8. Horwitz J. Alpha-crystallin can function as a molecular chaperone. *Proc Natl Acad Sci U SA*. 1992;89:10449–53.
9. Narberhaus F. Alpha-crystallin-type heat shock proteins: socializing mini-chaperones in the context of a multi-chaperone network. *Microbiol Mol Biol Rev*. 2002;66:64–93.

10. Panda AK, Nandi SK, Chakraborty A, Nagaraj RH, Biswas A. Differential role of arginine mutations on the structure and functions of α -crystallin. *Biochim Biophys Acta*. 2016;1860(1PtB):199–210.
11. Santhoshkumar P, Karmakar S, Sharma KK. Structural and functional consequences of chaperone site deletion in α -crystallin. *Biochim Biophys Acta*. 2016;1864:1529–38.
12. Mynampati BK, Muthukumarappa T, Ghosh S, Ram J. A silent mutation in human alpha-A crystallin gene in patients with age-related nuclear or cortical cataract. *Bosn J Basic Med Sci*. 2017;17:114.
13. Khoshaman K, Yousefi R, Niazi A, Oryan A, Moosavi-Movahedi AA, Kurganov BI. Importance of the positively charged residue at position 54 to the chaperone function, conformational stability and amyloidogenic nature of human α -crystallin. *J Biochem*. 2018;163:187–99.
14. Patel R, Zenith RK, Chandra A, Ali A. Novel Mutations in the Crystallin Gene in Age-Related Cataract Patients from a North Indian Population. *Mol Syndromol*. 2017;8:179–186.
15. Bhagyalaxmi SG, Srinivas P, Barton KA, Kumar KR, Vidyavathi M, Petrash JM, Bhanuprakash Reddy G, Padma T. A novel mutation (F71L) in α -crystallin with defective chaperone-like function associated with age-related cataract. *Biochim Biophys Acta*. 2009;1792(10):974–81.
16. Kimchi-Sarfaty C, Oh JM, Kim IW, Sauna ZE, Calcagno AM, Ambudkar SV, Gottesman MM. A “silent” polymorphism in the MDR1 gene changes substrate specificity. *Science*. 2007;315:525–8.
17. Supek F, Minana B, Valcarcel J, Gabaldon T, Lehner B. Synonymous mutations frequently act as driver mutations in human cancers. *Cell*. 2014;156:1324–35.
18. Das BK, Liang JJ, Chakrabarti B. Heat-induced conformational change and increased chaperone activity of lens α -crystallin. *Curr Eye Res*. 1997;16(4):303–9.
19. Lee JS, Satoh T, Shinoda H, Samejima T, Wu SH, Chiou SH. Effect of heat-induced structural perturbation of secondary and tertiary structures on the chaperone activity of α -crystallin. *Biochem Biophys Res Commun*. 1997;237:277–282.
20. Datta SA, Rao CM. Differential temperature-dependent chaperone-like activity of α A- and α B-crystallin homoaggregates. *J Biol Chem*. 1999;274:34773–8.
21. Tjondro HC, Xi YB, Chen XJ, Su JT, Yan YB. Membrane insertion of α -crystallin is oligomer-size dependent. *Biochem Biophys Res Commun*. 2016;473(1):1–7.
22. van den IJssel PR, Overkamp P, Knauf U, Gaestel M, de Jong WW. α -crystallin confers cellular thermoresistance. *FEBS Lett*. 1994;355:54–6.
23. Andley UP, Song Z, Wawrousek EF, Fleming TP, Bassnett S. Differential protective activity of α - and α B-crystallin in lens epithelial cells. *J Biol Chem*. 2000;275:36823–31.
24. Liu JP, Schlosser R, Ma WY, Dong Z, Feng H, Lui L, Huang XQ, Liu Y, Li DW. Human α - and α B-crystallins prevent UVA-induced apoptosis through regulation of PKC α , RAF/MEK/ERK and AKT signaling pathways. *Exp Eye Res*. 2004;79:393–403.
25. Yan Y, Qian H, Jiang H, Yu H, Sun L, Wei X, Sun Y, Ge H, Zhou H, Li X, Hashimoto T, Tang X, Liu P. Laminins in an in vitro anterior lens capsule model established using HLEB-3 cells. *Mol Med Rep*. 2018;17(4):5726–33.

26. Yoshitomi Y, Osada H, Satake H, Kojima M, Saito-Takatsuji H, Ikeda T, Yoshitake Y, Ishigaki Y, Kubo E, Sasaki H, Yonekura H. Ultraviolet B-induced Otx2 expression in lens epithelial cells promotes epithelial–mesenchymal transition. *Biol Open*. 2019; 18 (2).
27. Colognato H, Yurchenco PD. Form and function: the laminin family of heterotrimers. *Dev Dyn*. 2000; 218: 213–34.
28. Yan Y, Yu H, Sun L, Hanruo Liu C, Wang X, Wei F, Song H, Li H, Ge H, Qian X, Li X, Tang, Ping Liu. Laminin $\alpha 4$ overexpression in the anterior lens capsule may contribute to the senescence of human lens epithelial cells in age-related cataract. *Aging*. 2019; 11: 2699–723.
29. Yu H, Sun L, Cui J, Li Y, Wei Yu Y, Xi, Wang C, Song F, Jiang W, Liu Y, Ge H, Qian H, Li X, Tang X. Ping Liu. Three kinds of corneal host cells contribute differently to corneal neovascularization. *EBioMedicine*. 2019; 44: 542–53.
30. Christopher KL, Pedler MG, Shieh B, Ammar DA, Petrash JM, Mueller NH. Alpha-crystallin-mediated protection of lens cells against heat and oxidative stress-induced cell death. *Biochim Biophys Acta*. 2014; 1843(2): 309–15. doi:10.1016/j.bbamcr.2013.11.010.
31. Moon YW, Rao G, Kim JJ, Shim HS, Park KS, An SS, Kim B, Steeg PS, Sarfaraz S. Changwoo Lee L. LAMC2 enhances the metastatic potential of lung adenocarcinoma. *Cell Death Differ*. 2015; 22: 1341–52.
32. Pasupuleti N, Matsuyama S, Voss O, Doseff AI, Song K, Danielpour D, Nagaraj RH. The anti-apoptotic function of human αA -crystallin is directly related to its chaperone activity. *Cell Death Dis*. 2010; 1: e31.
33. Birlea SA, Costin GE, Roop DR, Norris DA. Trends in Regenerative Medicine: Repigmentation in Vitiligo Through Melanocyte Stem Cell Mobilization. *Med Res Rev*. 2017; 37: 907–35.
34. Kuphal S, Schneider N, Massoumi R, Hellerbrand C, Bosserhoff AK. UVB radiation represses CYLD expression in melanocytes. *Oncol Lett*. 2017; 14: 7262–8.

Tables

Table 1. Primers used in the present study.

Primers	Nucleotidesequence(5'-3')
CRYAA-exon1-F	GCTGGGGGCGGGCACTTG
CRYAA-exon1-R	TGGGGACACAGGCTCTCG
CRYAA-exon2-F	GGTGACCGAAGCATCTCTGT
CRYAA-exon2-R	CGTGACCCCCTTGTCTC
CRYAA-exon3-F	ACCCGGCCCCTGTGAGAG
CRYAA-exon3-R	AAAGGGAAGCAAAGGAAGACA
CRYAA-mRNA-F	TTTTGAGTATGACCTGCTGCC
CRYAA-mRNA-R	CAGAAGGTCAGCATGCCATC
GAPDH-mRNA-F	GCCAAGGTCATCCATGACAAC
GAPDH-mRNA-R	GTCCACCACCCTGTTGCTGTA

Figures

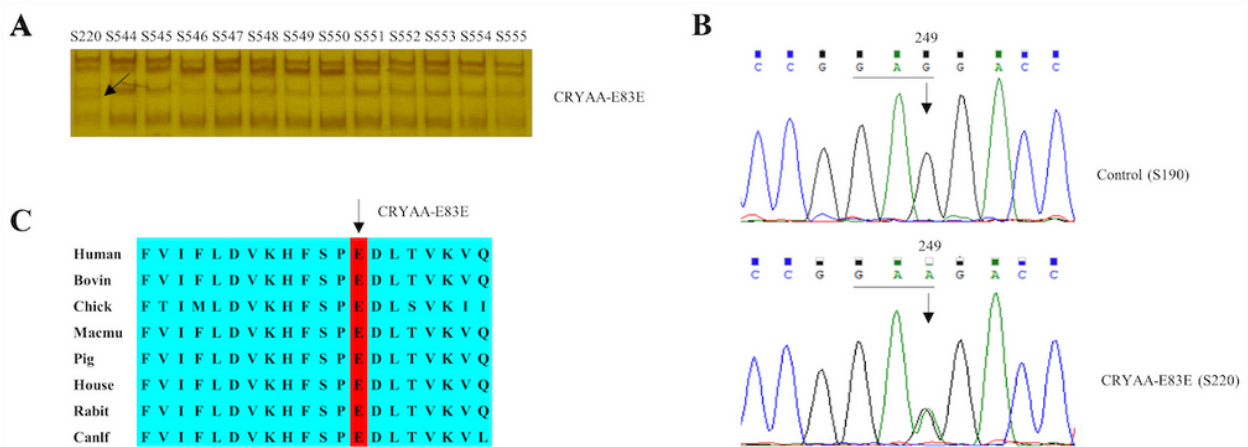


Figure 1

Screening and identification of CRYAA mutations in age-related cataract (ARC) patients. (A) Detection of CRYAA by PCR-SSCP assay. Dark arrow indicates the abnormal bands existed in affected individuals. (B) Sequence analysis of CRYAA in exon 2. The arrow showed a heterozygous G>A nucleotide change in exon 2 of CRYAA (c.249G>A), which leads to a silent mutation at codon 83 (p.E83E). (C) Multiple-sequence alignment in CRYAA at code 83 from different species.

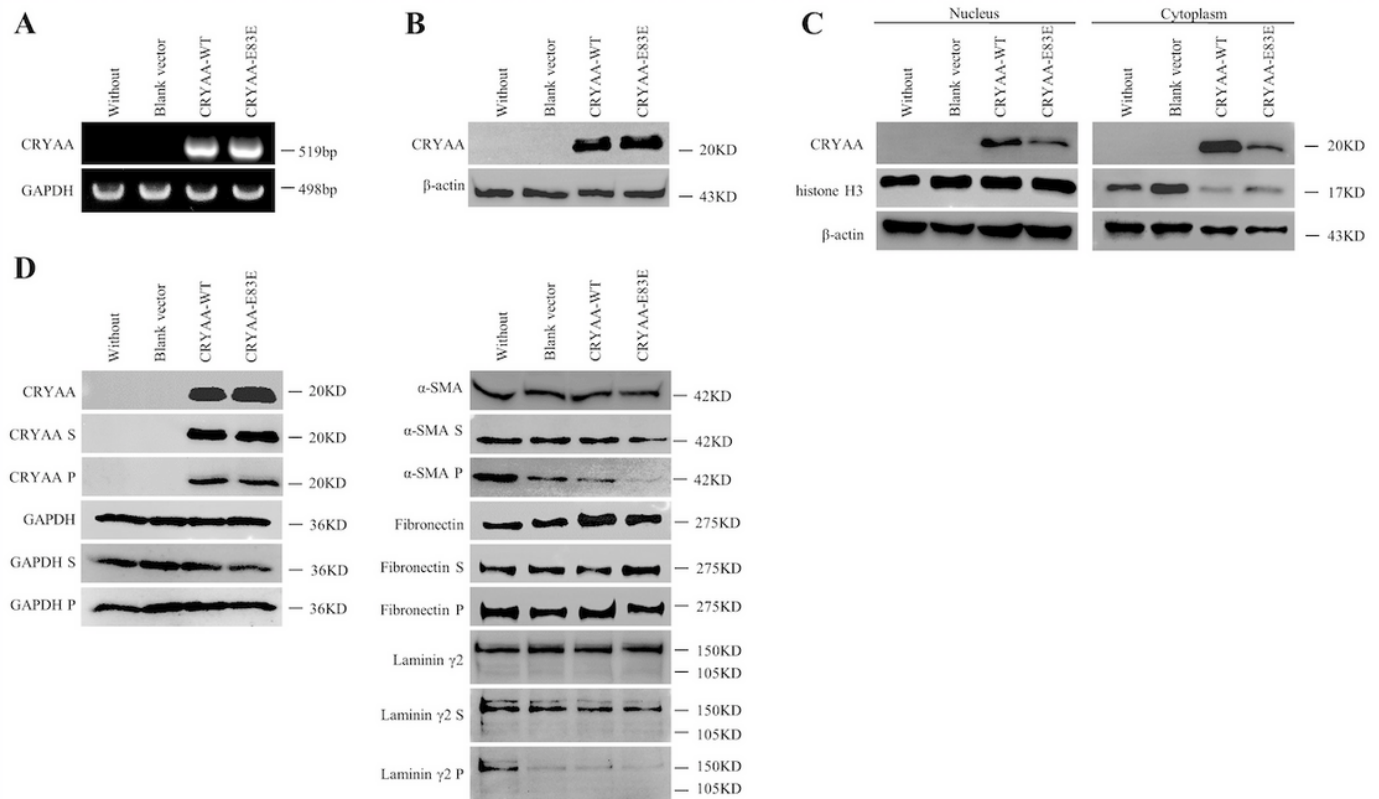


Figure 2

Protein expressions, distribution and chaperone function influenced by CRYAA-E83E. (A) Detection of CRYAA gene in HLE B-3 cells transfected with CRYAA-WT and CRYAA-E83E plasmid by RT-PCR. (B) Detection of CRYAA protein in HLE B-3 cell lysates transfected with CRYAA-WT and CRYAA-E83E plasmid by IB. (C) Detection of CRYAA and histone H3 in nuclear and cytoplasm of HLE B-3 cells transfected with CRYAA-WT and CRYAA-E83E plasmid by IB. (D) Detection of total, soluble (S) and insoluble (P) CRYAA, GAPDH, α-SMA, Fibronectin and laminin γ2 in HLE B-3 cells transfected with CRYAA-WT and CRYAA-E83E plasmid by chaperone function assay. Cell lysates incubated at 55°C for 3 h were separated into soluble (S) and insoluble (P) fractions by centrifugation.

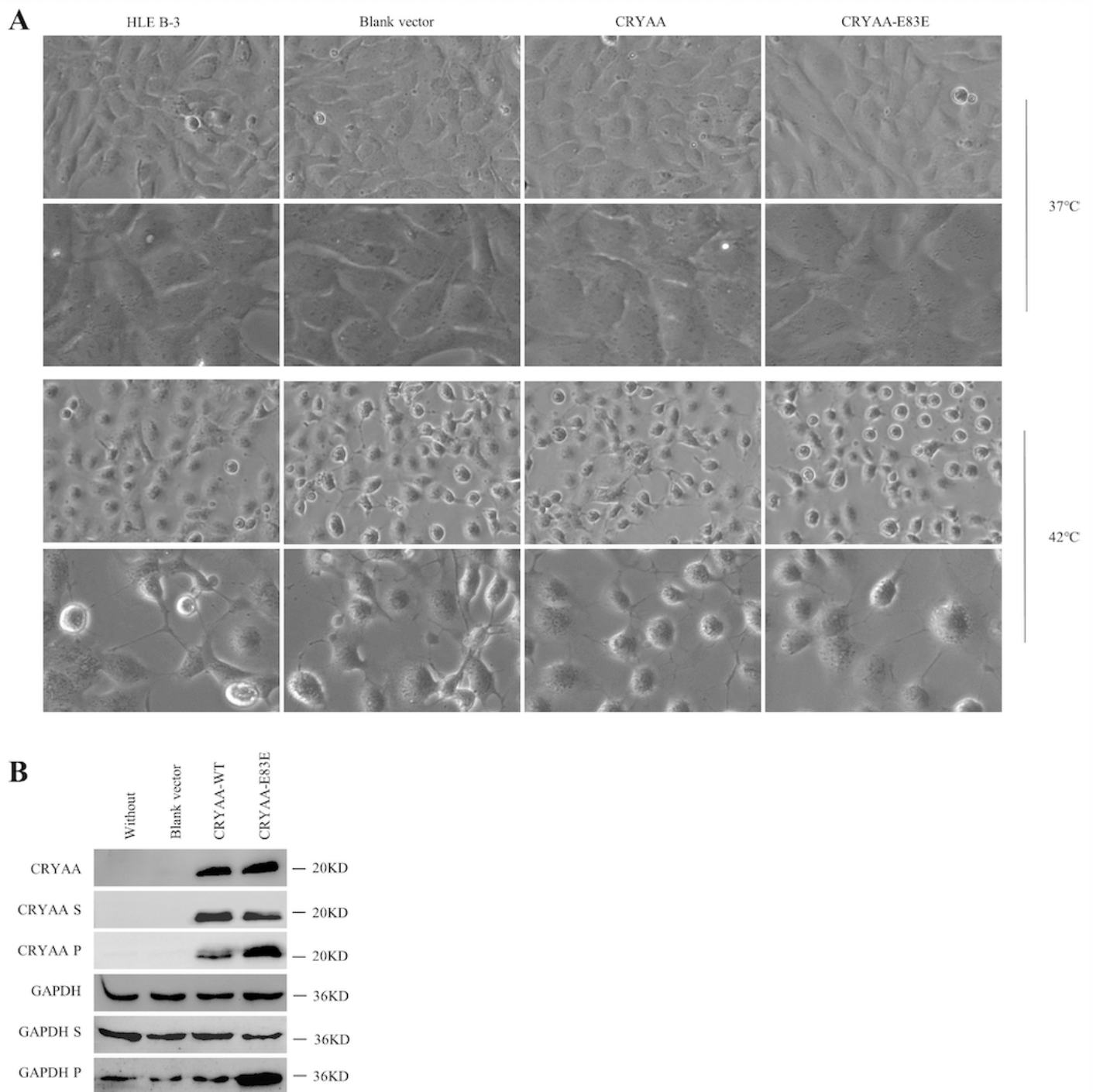


Figure 3

Morphology and chaperone function influenced by CRYAA-E83E treated with 42°C. HLE B-3 cells were cultured in medium at 37°C for 24 h, then changed into 42°C for 4 h, with those cultured at 37°C for 4 h as negative control. (A) Cell morphology. Magnification: 100x for the first and third row and 200x for the second and forth row. (B) Detection of total, soluble (S) and insoluble (P) CRYAA and GAPDH in HLE B-3

cells transfected with CRYAA-WT and CRYAA-E83E plasmid treated with 42°C by chaperone function assay. Cell lysates were treated as mentioned before.

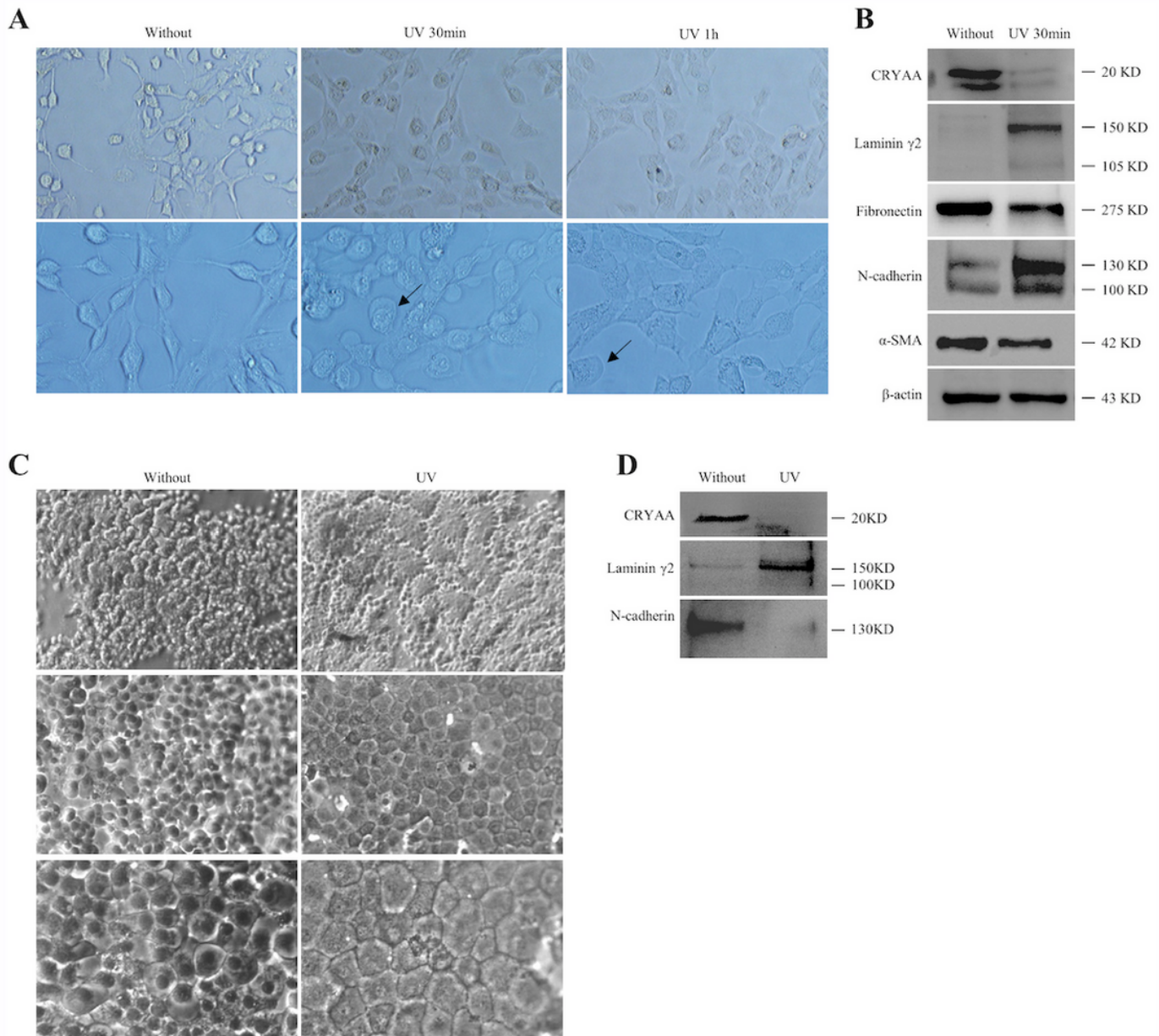


Figure 4

Morphology and protein expression of HLE B-3 cells and human anterior lens capsules treated by UV. HLE B-3 cells were treated with UV for 30 min or 1 h, with those cultured at room temperature for 1 h as negative control (without). (A) Morphology of HLE B-3 cells. Magnification: 100x for upper row and 200x for lower row. Arrows indicated the apoptotic cells. (B) Detection of CRYAA, laminin γ 2, Fibronectin, N-cadherin and α -SMA in HLE B-3 cells treated with UV by IB. (C) Morphology of human lens epithelial cells. Human anterior lens capsules were first treated with UV for 1 h and then cultured in medium at 37°C for 24 h, and then treated with UV for 30 min. Capsules without treatment with UV were as negative control

(without). Magnification: 40x for upper row, 100x for middle row and 200x for lower row. (D) Detection of CRYAA, laminin γ 2 and N-cadherin in human anterior lens capsules treated with UV by IB.

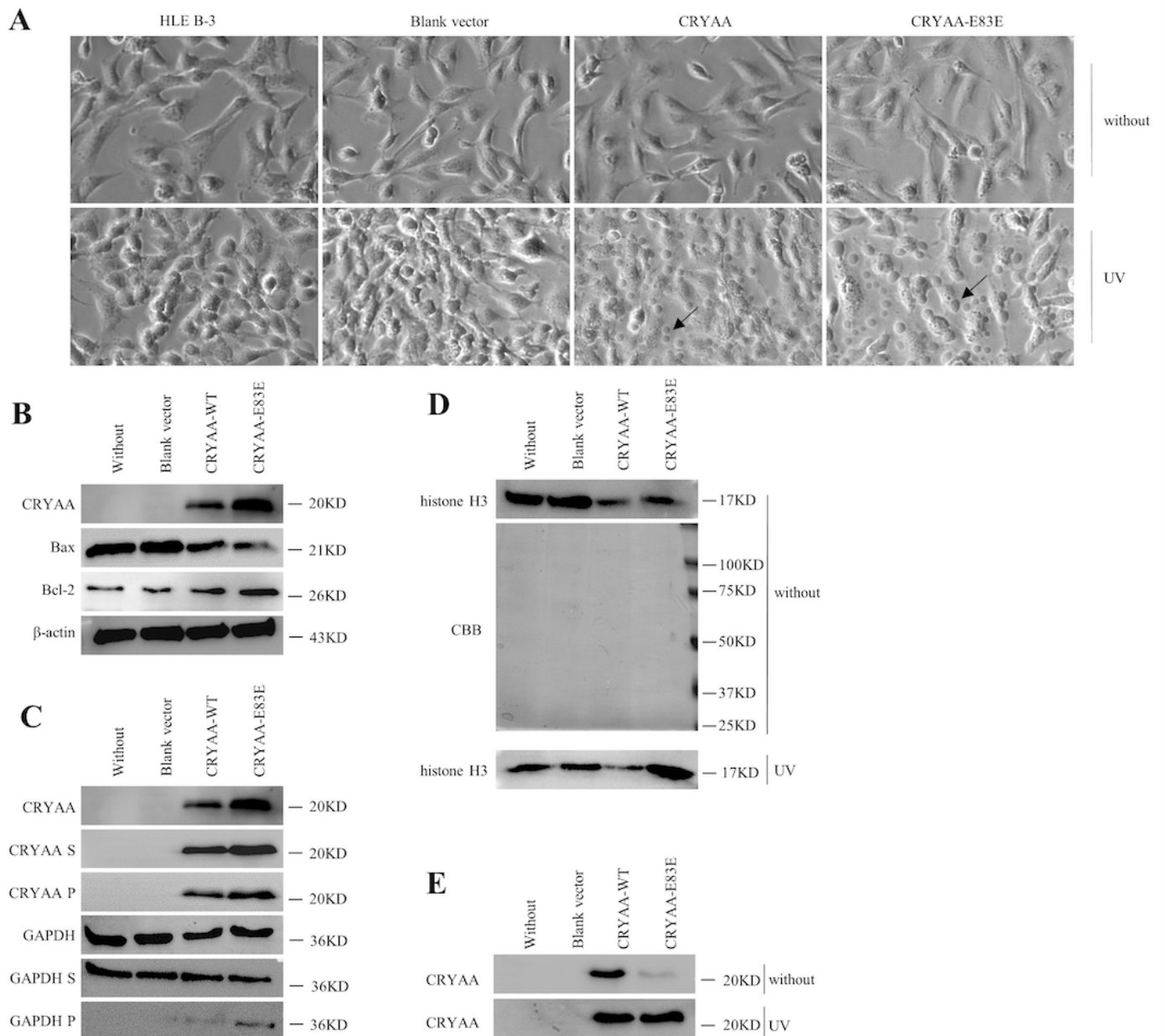


Figure 5

Morphology and chaperone function influenced by CRYAA-E83E treated with UV. HLE B-3 cells were cultured in medium for 24 h, then treated with UV for 30 min, with those cultured at room temperature for 30 min as negative control (without). (A) Cell morphology. Magnification: 200x. Arrows indicated the apoptotic bodies. (B) Detection of CRYAA, Bax and Bcl-2 in HLE B-3 cells transfected with CRYAA-WT and CRYAA-E83E plasmid by IB. (C) Detection of total, soluble (S) and insoluble (P) CRYAA and GAPDH in HLE B-3 cells transfected with CRYAA-WT and CRYAA-E83E plasmid by chaperone function assay. (D)

Detection of histone H3 by IB (top), and total proteins by CBB staining (bottom) in UV treated basement membranes of HLE B-3 cells transfected with CRYAA-WT and CRYAA-E83E plasmid. (E) Detection of CRYAA in HLE B-3 cell supernatant transfected with CRYAA-WT and CRYAA-E83E plasmid by IB.

Supplementary Files

This is a list of supplementary files associated with this preprint. Click to download.

- [supplement1.doc](#)